Available online at www.sciencedirect.com
ScienceDirect
Polymer 48 (2007) 3192–3200
polymer
www.elsevier.com/locate/polymer

Micellar morphologies of self-associated diblock copolymers in acetone solution

Pao-Hsiang Tung, Shiao-Wei Kuo, Shih-Chien Chen, Chen-Lung Lin, Feng-Chih Chang*

Institute of Applied Chemistry, National Chiao-Tung University, Hsinchu, Taiwan

Received 6 February 2007; received in revised form 24 March 2007; accepted 26 March 2007
Available online 5 April 2007

Abstract

We describe the synthesis and solution morphologies of poly(vinyl phenol-*b*-styrene) (PVPh-*b*-PS) micelles and the effects that changing the copolymer composition and concentration have on self-assembly structures of PVPh-*b*-PS in acetone (a good solvent for PVPh). These PVPh-*b*-PS copolymers aggregated into spherical, rod-like, and vesicular morphologies. The transformations of the PVPh-*b*-PS block copolymer micelles in acetone depended on a number of parameters, including the relative block lengths, their concentrations, and the degree of self-association through hydrogen bonding of the coronal PVPh chains. We also investigated the morphologies of the micelles formed from acetone solutions of poly(4-*tert*-butoxystyrene-*b*-styrene) (P*t*BOS-*b*-PS) copolymers having the same degree of polymerization as the precursor of PVPh-*b*-PS copolymer before hydrolysis reaction. Our results indicate that the micelles formed from PVPh-*b*-PS copolymers in acetone were more complicated than those prepared from P*t*BOS-*b*-PS copolymers in acetone because hydrogen bonding occurs in the micelle corona of the PVPh block. Finally, we also discussed the morphology transition when the self-association hydrogen bonding of PVPh block was destroyed by adding proton acceptor poly(4-vinylpyridine) (P4VP).

Keywords: Block copolymer; Self-assembly; Micelle

1. Introduction

Block copolymers attract a considerable amount of attentions because of their abilities to self-assemble in the solid state or in solutions to form a range of morphologies (e.g., spheres, cylinders, and lamellae) of various sizes [1–5]. The shapes and sizes are determined by a number of factors, such as relative block lengths, the chemical nature of blocks, and the type of solvents. During the past decade, many publications have described the synthesis of block copolymer aggregate morphologies in solution [6–12]. In most of these investigations, the polymeric micelles were dissolved at the molecular level in various solvents. Selective solvents often lead to the formation of micelles, where the insoluble or less soluble parts of the block copolymers form core domains that are surrounded by a highly swollen corona of the soluble blocks. Depending upon the interactions of the corona chains and the relative compositions of the block copolymers, micelles of various shapes can be formed, most often with spherical or cylindrical morphologies. Stable aggregates with a range of morphologies are obtained under various conditions [13,14]. For instance, the preparation of asymmetric poly(styrene-*b*-acrylic acid) diblock copolymer [15] (PS-*b*-PAA) aggregates is performed by dissolving the polymer in a common solvent (a good solvent for both, e.g., DMF or dioxane) and then adding the selective good solvent for the short blocks (e.g., water for PAA) to induce aggregation of the insoluble blocks. Direct dissolution in single solvent is possible to form star micelles if the hydrophilic block is relatively long in relation to the hydrophobic block. The preparation of crew-cut aggregates through a direct dissolution in a single solvent is difficult, however, a long length of the hydrophobic core block makes the polymer insoluble in polar solvents.

* Corresponding author. Tel./fax: +886 3 5131512.
E-mail address: changfc@mail.nctu.edu.tw (F.-C. Chang).

0032-3861/$ - see front matter © 2007 Elsevier Ltd. All rights reserved.
doi:10.1016/j.polymer.2007.03.071

To date, only a few reports [16,17] discuss the transformation of one crew-cut micellar morphology into another when using a single-solvent method and changing temperature. Eisenberg et al. first prepared the PS-*b*-PAA crew-cut aggregates by dissolving the copolymer at elevated temperature and then cooling [16]. Liu et al. reported the multiple morphologies and transformations of PS-*b*-P4VP in low-alkanol solvents and investigated the influence that the rate of cooling had on the resulting morphologies [17]. It is well established that the transformation of spheres to rods, to tire-shaped large compound micelles, or to spherical shaped large compound micelles is determined by a balance between three main effects: stretching of the core-forming blocks, inter-coronal interactions, and the interfacial energy between the solvent and the micellar core [14]. By tuning one of these three factors, the forces balancing the micelles can be upset, leading to a transformation from one morphology into another.

In this paper, we report the synthesis of poly(vinyl phenol-*b*-styrene) (PVPh-*b*-PS) diblock copolymers through sequential anionic polymerization, the preparation of the block copolymer micelles using a single solvent (acetone) method, and the preparation of various polymeric morphologies upon changing the relative block lengths and concentrations. To prove formation of hydrogen bonds in the micellar corona is an important factor affecting micelle formation. We have also investigated the micellar structures of poly(4-*tert*-butoxystyrene-*b*-styrene) (P*t*BOS-*b*-PS) block copolymers, the precursors of the corresponding PVPh-*b*-PS diblock copolymer before hydrolysis (without hydroxyl group). We observed that the different hydrogen bonding interaction abilities of the PVPh-*b*-PS and P*t*BOS-*b*-PS diblock copolymers led to the formation of different micellar morphologies in acetone solution. In addition, we also add a small amount of proton acceptor, poly(4-vinylpyrindine), to decrease the strength of self-association hydrogen bonding of PVPh. Totally different micellar morphologies between PVPh-*b*-PS and PVPh-*b*-PS/P4VP are due to the intermolecular hydrogen bonding between PVPh and P4VP.

2. Experimental part

2.1. Materials

Tetrahydrofuran (THF) was dried under reflux in the presence of potassium and a small amount of benzophenone until a purple color developed; it was distilled prior to use. Initiator, *sec*-butyl lithium (1.3 M in cyclohexane), styrene (99%), and 4-*tert*-butoxystyrene (*t*BOS, 99%) were purchased from Aldrich. These monomers were purified through vacuum distillation first over calcium hydride (CaH_2) and then in the presence of triethylaluminum, prior to use.

2.2. Syntheses of block copolymers

The P*t*BOS-*b*-PS diblock copolymers were synthesized through sequential anionic polymerization of *t*BOS and styrene using *sec*-butyl lithium as the initiator; the synthesis is presented in Scheme 1 [18,19]. The polymerization was performed in THF at −78 °C under an inert atmosphere. The 4-*tert*-butoxystyrene monomer was polymerized first for 2 h; an aliquot of the poly(4-*tert*-butoxystyrene) was isolated for analysis after termination of the reaction using degassed methanol. Styrene monomer was then introduced into the reactor and the reaction was terminated again with degassed methanol after 2 h. A series of diblock copolymers were obtained by withdrawing aliquots of the mixtures after each styrene monomer addition. The degree of polymerization of the P*t*BOS blocks and the polydispersities of the homopolymers and diblock copolymers were determined using gel permeation chromatography (GPC). The P*t*BOS blocks in the copolymers were hydrolyzed to their acid form in dioxane using conc. HCl as the catalyst. Detailed descriptions of the procedures are available elsewhere [19]. The resulting PVPh-*b*-PS diblock copolymers were subjected to two dissolve (THF)/precipitate (methanol/water) cycles and then purified through Soxhlet extraction with water for 72 h prior to being dried under vacuum at 80 °C.

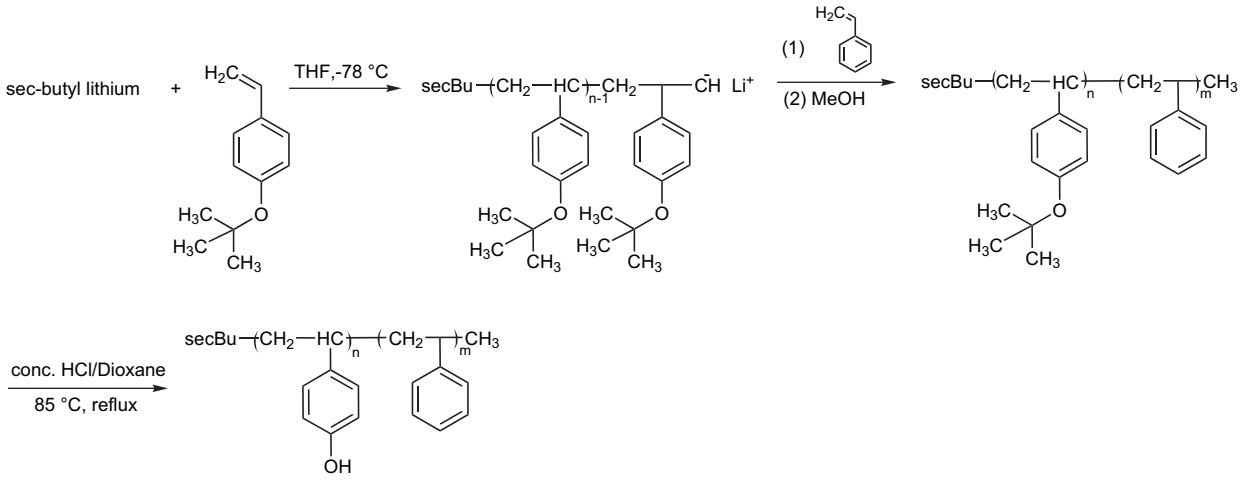

Scheme 1. Synthesis of poly(vinyl phenol-*b*-styrene) diblock copolymer through anionic polymerization.

2.3. Micellization procedures

Acetone was chosen as a selective solvent to prepare the micellar solutions. Both PVPh and P*t*BOS are soluble in acetone, but PS is relatively less soluble. Herein, we prepared star micelles and crew-cut aggregates in acetone solution by varying the block copolymer compositions. Star micelles and crew-cut aggregates were obtained by simply dissolving these copolymers in acetone. These polymeric micellar aggregates possessed a corona of PVPh or P*t*BOS and a core of PS.

2.4. Characterizations

The molecular weight and molecular weight distribution were determined by gel permeation chromatography (GPC) using a Waters 510 HPLC equipped with a 410 differential refractometer, a refractive index (RI) detector, and a UV detector. Three Ultrastyragel columns (100, 500, and 103 Å) were connected in series in the order of increasing pore sizes; DMF was used as the eluent at a flow rate of 0.6 mL/min. Polystyrene standards were employed for molecular weight calibration. ^{1}H and ^{13}C NMR spectra were recorded in d_6-DMF using an INOVA 500 (500 MHz) spectrometer; the solvent signal was chosen as the internal standard. Fourier transform infrared (FTIR) spectra were recorded at 25 °C using a Nicolet AVATAR 320 FTIR spectrometer; polymer films were cast onto KBr pellets from THF solution. All FTIR spectra were obtained within the range 4000–400 cm^{-1}; 32 scans were collected at a resolution of 1 cm^{-1} while samples were purged with nitrogen to ensure that the films remained dry. Transmission electron microscopic (TEM) images were obtained using a Hitachi H-7500 instrument with an accelerating voltage of 100 kV. The TEM samples were deposited from acetone solutions onto carbon-coated copper grids. After drying, the samples were stained with ruthenium tetraoxide (RuO_4). Atom force microscopic (AFM) images were obtained using a scanning probe microscope (Digital Instrument, MultiMode) operated in the tapping mode. Samples for AFM measurements were prepared by casting the suspensions onto mica and then drying them in a constant humidity oven at 25 °C for 24 h.

3. Results and discussion

3.1. Synthesis and hydrolysis of diblock copolymers

The PVPh-*b*-PS diblock copolymers were prepared through the living anionic polymerization of P*t*BOS-*b*-PS and subsequent hydrolytic deprotection. The hydrolysis of the P*t*BOS-*b*-PS copolymers was performed at 85 °C in dioxane in the presence of conc. HCl, giving the PVPh-*b*-PS diblock copolymers quantitatively (Scheme 1). Fig. 1 displays GPC traces of the $PVPh_{18}$-*b*-PS_{124}, the protected $PtBOS_{18}$-*b*-PS_{124}, and the P*t*BOS prepolymer; all indicate a narrow molecular weight distribution (<1.2). Although the block copolymers we prepared from the P*t*BOS provided highly symmetrical and monomodal GPC traces, the PVPh-*b*-PS copolymer exhibited

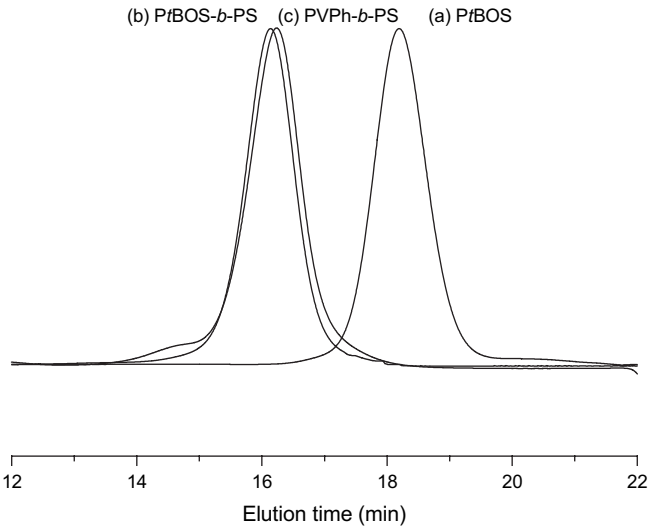

Fig. 1. GPC traces of $PVPh_{18}$-*b*-PS_{124} block copolymers. (a) Poly(4-*tert*-butoxystyrene) (P*t*BOS, $M_n = 3100$, PDI = 1.08); (b) poly(4-*tert*-butoxystyrene-*b*-styrene) (P*t*BOS-*b*-PS, $M_n = 16\,000$; PDI = 1.09); (c) poly(vinyl phenol-*b*-styrene) (PVPh-*b*-PS, $M_n = 15\,000$, PDI = 1.09).

a slightly broader polydispersity ($M_w/M_n = 1.15$) than did the corresponding P*t*BOS-*b*-PS copolymer ($M_w/M_n = 1.09$). This broader polydispersity is likely to be the result of a "high molecular weight shoulder" probably because of polymer–stationary phase interactions arising from inter-chain hydrogen bonding [20,21]. This diblock copolymer system has been investigated previously [20–22]; living anionic polymerization of the protected hydroxystyrene [19–24] and styrene [20–22,25] monomers has also been documented well. In general, to obtain a monodisperse PVPh block, it is necessary to protect the hydroxyl group prior to polymerization to avoid termination of the living chain end. Various protecting groups, including *tert*-butyl ether [21,22] and *tert*-butyldimethylsilyl [20] units, have been used to block the hydroxyl group during anionic polymerization. In this study, we used the *tert*-butyl ether-protected monomer because of its ease of hydrolysis and ready availability. The FTIR spectrum (Fig. 2b) of the resulting block copolymer after hydrolysis clearly displays a broad peak at 3450 cm^{-1} indicating the presence of the hydroxyl groups.

The total removal of the protective groups to form the desired phenolic hydroxyl groups was verified by ^{1}H and ^{13}C NMR spectroscopies. Fig. 3a and b displays typical ^{1}H NMR spectra of these diblock copolymers before and after deprotection, respectively. The signal at 1.29 ppm corresponds to the *tert*-butyl groups of the P*t*BOS-*b*-PS copolymer (in $CDCl_3$). This characteristic peak disappeared essentially in the hydrolyzed block copolymer; only the polymer backbone protons appear in the region between 1 and 2 ppm. In addition, a peak (7.9 ppm) corresponding to the protons of the hydroxyl groups appears after hydrolysis reaction. Fig. 3c indicates that the signal of the quaternary carbon atoms of the *tert*-butyl groups in the P*t*BOS segment is located at 78.0 ppm [26]. After hydrolysis reaction, no signal remains for these *tert*-butyl groups in the ^{13}C NMR spectrum of the PVPh-*b*-PS

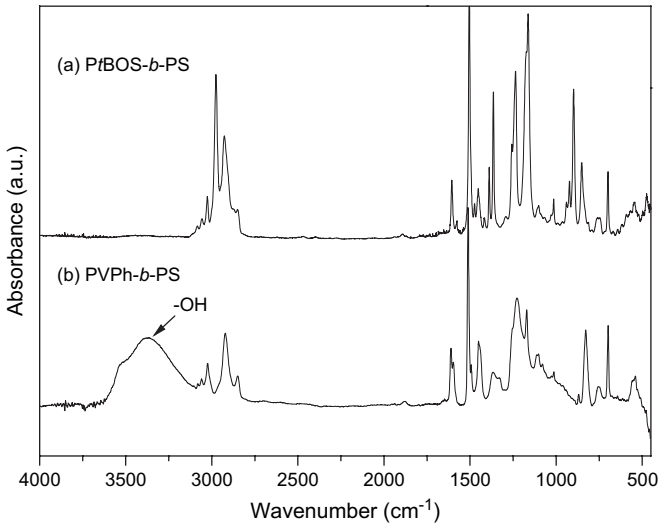

Fig. 2. IR spectra of (a) P*t*BOS-*b*-PS and (b) PVPh-*b*-PS recorded at room temperature.

copolymer (Fig. 3d), indicating that the hydrolysis reaction was complete. We determined the compositions of the PVPh-*b*-PS block copolymers from the relative intensities of the aromatic ring (6.3–7.2 ppm) and hydroxyl group (7.7–7.9 ppm) protons of the VPh units in the ^{1}H NMR spectra. We calculated the molecular weights and PVPh/PS ratios of the various copolymers from these ^{1}H NMR spectra and compared these values with those obtained through GPC (Table 1). The polymers are denoted as $PVPh_n$-*b*-PS_m, where *n* and *m* stand for the degree of polymerizations of PVPh and PS blocks, respectively.

3.2. Micellar characteristics in acetone

Polymeric micelles of different morphologies from the PVPh-*b*-PS diblock copolymers were obtained through the use of a single-solvent method. PVPh is soluble in acetone, but PS is only slightly soluble. The PVPh-*b*-PS diblock copolymers containing PVPh contents ranging from 11% to 79% dissolved completely in dilute acetone solution (0.01 wt%) at 40 °C. We investigated the effects that the diblock copolymer compositions and concentrations had on the aggregation behavior.

Fig. 4 displays TEM images of the various morphologies formed from PVPh-*b*-PS copolymers having different PVPh fractions, but the same concentration (0.01 wt%) in acetone solution. Nano-spherical micelles of PVPh-*b*-PS formed are shown in Fig. 4A–D. When the PVPh to PS block length ratio was decreased further, such as in the $PVPh_{35}$-*b*-PS_{372} ($f_{PVPh} = 0.11$) system, the aggregates transformed into coexisting short rod-like micelles and spherical micelles (Fig. 4E). These short rod-like micelles possessed a relatively narrow distribution of diameters, but were widely variable in their lengths. These morphologies transit from spherical micelles to coexisting short rod-like and spherical micelles by decreasing the molar ratio of PVPh. It is well known that several factors influence the morphology of block copolymer

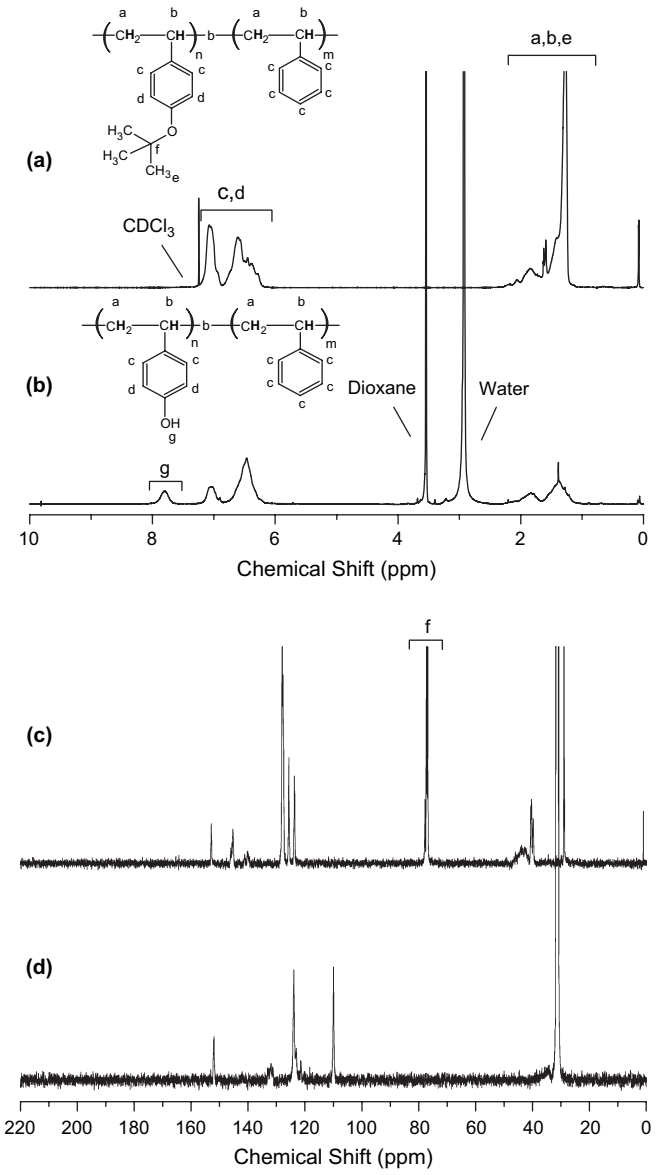

Fig. 3. ^{1}H NMR spectra of (a) P*t*BOS-*b*-PS (before hydrolysis) in $CDCl_3$ and (b) PVPh-*b*-PS (after hydrolysis) in 1,4-dioxane-d_8; ^{13}C NMR spectra of (c) P*t*BOS-*b*-PS (before hydrolysis) in $CDCl_3$ and (d) PVPh-*b*-PS (after hydrolysis) in 1,4-dioxane-d_8.

Table 1
Molecular characterization of PVPh-*b*-PS diblock copolymers prepared by anionic polymerization

Precursor copolymer	Copolymer	Total M_n[a] (g/mol)	Composition of PVPh[b] (mol%)	M_w/M_n[a]
P*t*BOS$_{35}$-*b*-PS$_{372}$	PVPh$_{35}$-*b*-PS$_{372}$	45 000	11	1.17
P*t*BOS$_{18}$-*b*-PS$_{124}$	PVPh$_{18}$-*b*-PS$_{124}$	16 000	18	1.09
P*t*BOS$_{44}$-*b*-PS$_{195}$	PVPh$_{44}$-*b*-PS$_{195}$	28 000	30	1.08
P*t*BOS$_{107}$-*b*-PS$_{163}$	PVPh$_{107}$-*b*-PS$_{163}$	36 000	41	1.15
P*t*BOS$_{116}$-*b*-PS$_{72}$	PVPh$_{116}$-*b*-PS$_{72}$	28 000	65	1.12
P*t*BOS$_{89}$-*b*-PS$_{27}$	PVPh$_{79}$-*b*-PS$_{27}$	18 500	79	1.13
P*t*BOS$_{85}$-*b*-PS$_{10}$	PVPh$_{85}$-*b*-PS$_{10}$	16 000	90	1.10

[a] Polydispersity index and molecular weight, measured by GPC, of the whole diblock copolymer in the form of P*t*BOS-*b*-PS.
[b] Obtained from ^{1}H NMR spectra.

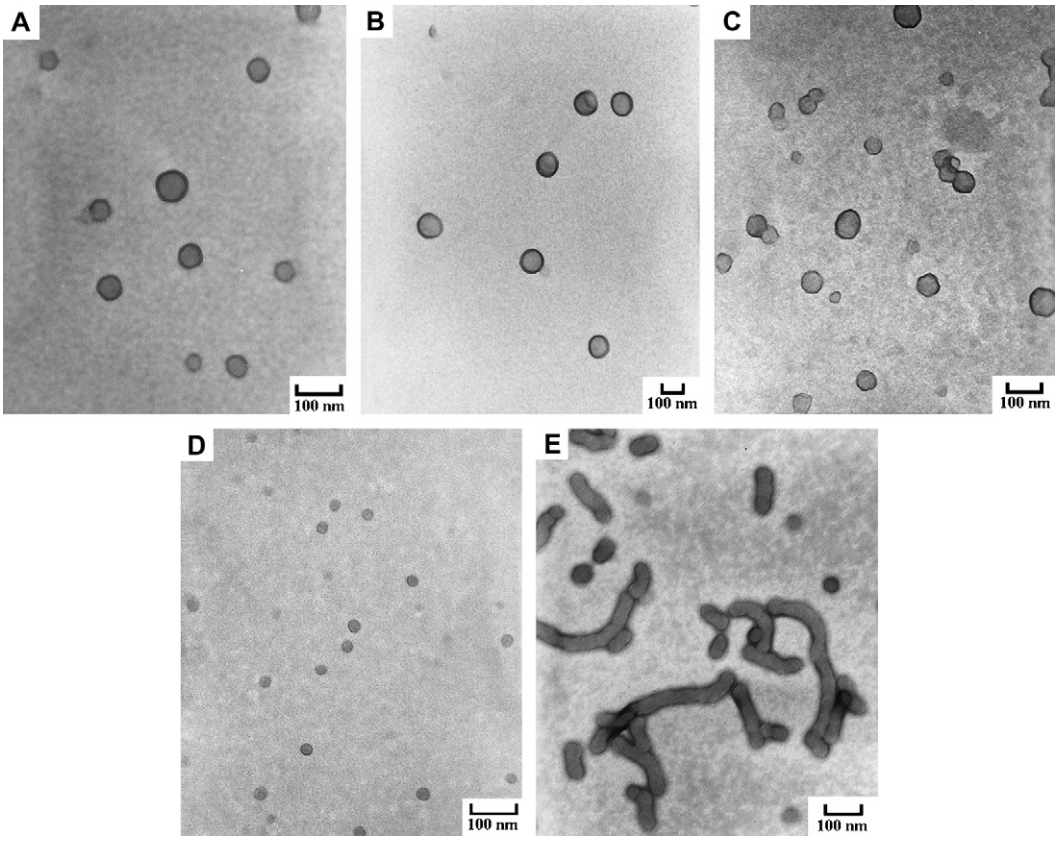

Fig. 4. TEM images of the morphologies of the polymeric micelles prepared from 0.01 wt% PVPh-*b*-PS copolymers in acetone. (A) $PVPh_{85}$-*b*-PS_{10}, (B) $PVPh_{79}$-*b*-PS_{27}, (C) $PVPh_{116}$-*b*-PS_{72}, (D) $PVPh_{18}$-*b*-PS_{124}, and (E) $PVPh_{35}$-*b*-PS_{372}.

aggregates in a solution [13,14]. For example, the free energies of aggregation are affected by the inter-coronal chain interaction, the core–coronal interfacial energy, and the degree of core-chain stretching. Here, the PVPh moieties are capable of forming specific interactions via self-association through hydrogen bonding and thus the existence of hydrogen bonds plays an important role in determining the morphology of the micellar corona. Therefore, hydrogen bond formation is an additional driving force that affects micelle formation in our present system. For example, when the PVPh blocks were relatively long, the block copolymer tended to form a spherical structure, which is similar with poly(methyl methacrylate-*b*-acrylic acid) (PMMA-*b*-PAA) in aqueous solution [27]. A possible reason for this phenomenon is that the self-association hydrogen bonding of the PVPh block is more favorable than inter-association hydrogen bonding between the carbonyl group of acetone and the hydroxyl groups of PVPh [28,29]. Therefore, the intra-chain hydrogen bonding of PVPh tends to result in aggregation and the formation of a spherical structure at a relatively higher PVPh content. When the PVPh to PS block length ratio decreases, however, the influence of the self-association hydrogen bonding of PVPh decreases and, thus, the block copolymer aggregates display similar crew-cut aggregation behaviors (nanosphere or rod-like micelles), similar to that of other systems such as the PS-*b*-PAA, in DMF/water solution [13–15]. In addition, the surface per corona chain will usually decrease as the morphology changes from spherical to rod-like micelle. As soluble blocks are relatively long, it favors the formation of spherical micelle because the density of corona chain on the core surface is higher. When soluble blocks are gradually decreased, the surface per corona chain is decreased and the morphology changes from sphere to cylinder.

The final equilibrium morphology depends not only on the relative ratio of the length of the insoluble/soluble block, but also on the concentration of the block copolymer. Fig. 5 displays TEM and AFM images of the micelles prepared from $PVPh_{35}$-*b*-PS_{372} ($f_{PVPh} = 0.11$) at various concentrations in acetone. It is interesting to note that the morphology of the $PVPh_{35}$-*b*-PS_{372} shifted from spherical to rod-like upon increasing the concentration. When the copolymer concentration was extremely low (0.001 wt%), we observed only spheres (Fig. 5A); the cylindrical micelles appeared after increasing the concentration. The spherical and cylindrical micelles coexisted at 0.01 and 0.025 wt% (Fig. 5B and C, respectively). Two spherical end caps are clearly resolved for each cylindrical micelle; because the diameters of these cylinders were equal to the diameters of individual spherical micelles, we suggest that these cylindrical micelles formed through coalescence of individual elementary spherical micelles. As the concentration increased further to 0.15 wt%, the solution turned from completely colorless and transparent to slightly bluish, indicating that either the micelles became larger or the copolymer became less soluble in acetone. Fig. 5D and E indicates that

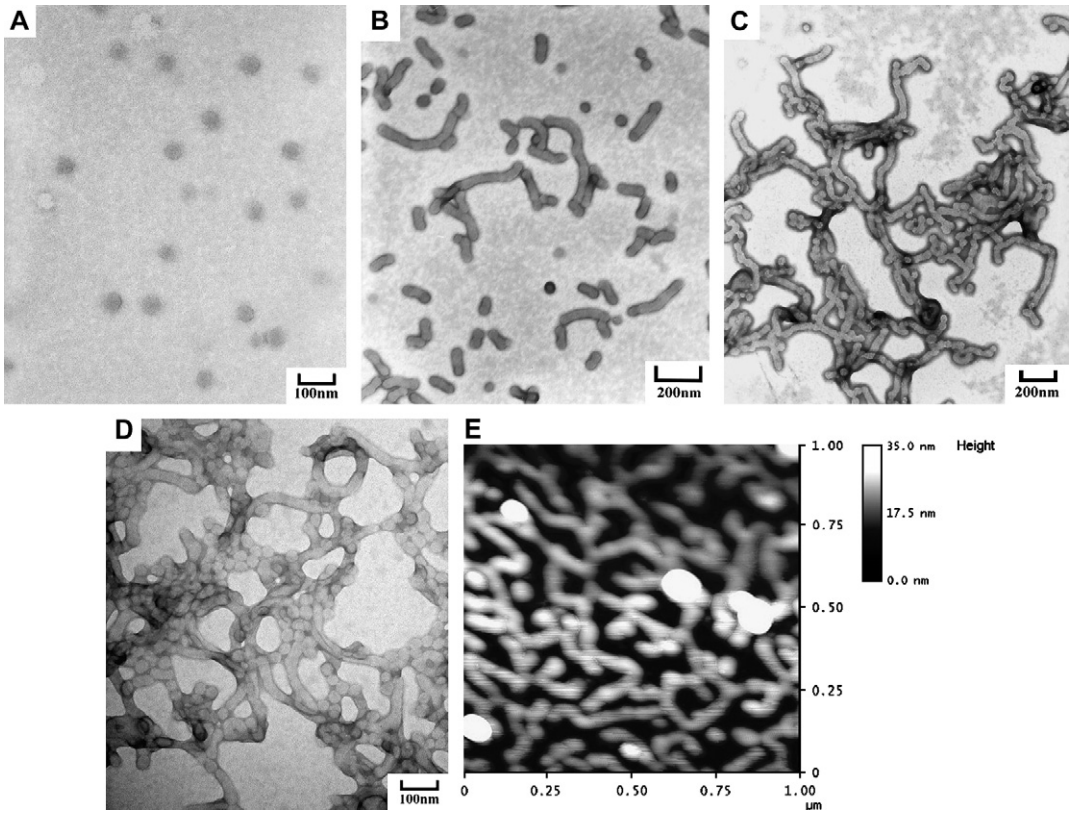

Fig. 5. TEM images of the morphologies of the aggregates prepared from $PVPh_{35}$-*b*-PS_{372} at (A) 0.001, (B) 0.01, (C) 0.025, (D) 0.15 wt% and (E) AFM image of 0.15 wt% in acetone.

worm-like micelles and pearl-necklace structures coexisted at 0.15 wt%. Most of the worm-like micelles exhibited a wide range of lengths, but their cross-sectional diameters were nearly constant (ca. 45 nm, as measured using TEM).

Another approach toward promoting the growth of $PVPh_{35}$-*b*-PS_{372} micelles is to change its concentration using dynamic light scattering (DLS). The CONTIN profiles for the $PVPh_{11}$-*b*-PS_{89} micelles indicate that both the size and polydispersity were concentration-dependent (see Supplementary data). We discovered that the hydrodynamic diameter of the $PVPh_{35}$-*b*-PS_{372} micelles increased upon increasing the block concentration. Such sphere-to-rod transition phenomena have been reported recently elsewhere [30–32]. Burke et al. described the sphere-to-rod transitions of a ternary system of PS_{310}-*b*-PAA_{52}/dioxane/water [31], but there are certain differences between their system and ours. The sphere-to-rod transition was accomplished by changing the selective solvent, water, in ternary system described by Burke et al. In our case, the crew-cut aggregates were formed by simply changing the concentration of the diblock copolymer within a single solvent; i.e., in the $PVPh_{35}$-*b*-PS_{372}/acetone system, we achieved the sphere-to-rod transition simply by increasing the copolymer concentration.

The mechanism of formation in our system remains unclear, although we believe that adhesive contact and fusion of spheres are involved. By increasing the copolymer concentration, the solubility of the core section of the micelles is reduced, as would be expected. Therefore, stretching of the PS block must be thermodynamically unfavorable, which suggests that the micellar morphology changes from spherical to rod-like because of an overall decrease in the free energy of micellization [33]. Another possible mechanism involves adhesive collisions and repeated aggregation of small spherical micelles to form the rod-like micelles [34]. This morphological transition may be caused by an alternation in the nature of the local hydrogen interactions within the nanostructure; the coronal PVPh chains tend to attract one another through strong self-associative hydrogen bonding. Similarly, Minatt et al. reported the morphologies of the micelles formed from linear and cyclic PS-*b*-PI copolymers ($f_{PS} = 0.78$) in heptane [35]; they observed the sphere-to-rod transition phenomena occurred upon changing the concentration of only the cyclic PS-*b*-PI micelles. They suggested that these giant worm-like micelles created from the cyclic copolymer chains arose from the self-assembly of ''sunflower-like'' micelles [35–38]. We speculate that strong self-associative hydrogen bonding of these coronal PVPh chains must play an important role in our single-solvent system. The $PVPh_{35}$-*b*-PS_{372} system did not self-assemble into classical spherical micelles in dilute solution; instead, it tended to form sunflower-like micelles. In our case, the worm-like micelles originated from repeated self-assembly of a series of sunflower-like spherical micelles (see Scheme 2). We also observed (Fig. 6) such a concentration on the micellar morphology transition of $PVPh_{18}$-*b*-PS_{124} ($f_{PVPh} = 0.18$). The micellar morphology changed from spherical-to-vesicle upon increasing the micellar concentration.

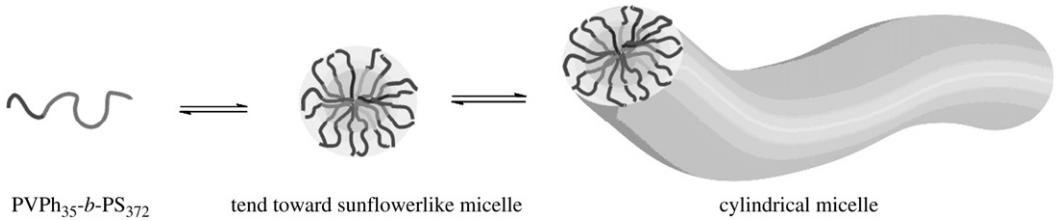

Scheme 2. Models of the process of micelle formation for the $PVPh_{35}$-*b*-PS_{372} diblock copolymer in acetone solution.

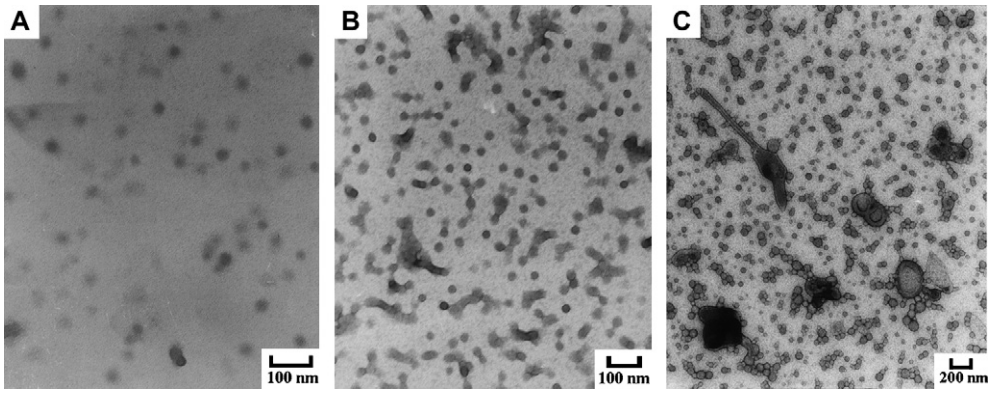

Fig. 6. TEM images of the $PVPh_{18}$-*b*-PS_{124} assemblies formed in acetone at concentrations of (A) 0.01, (B) 0.02, and (C) 0.03 wt%.

To demonstrate the importance of self-associative hydrogen bonding in the PVPh-*b*-PS/acetone system, we also compared the micelle formation of the two block copolymers, $PVPh_{35}$-*b*-PS_{372} and P*t*BOS_{35}-*b*-PS_{372}, having identical degrees of polymerization, in acetone solution. The solubility parameter of acetone [39] is 20.4 and those of homopolymers of PS [40], PVPh [29], and P*t*BOS [39] are 18.0, 21.6, and 20.5 $MPa^{1/2}$, respectively. From a comparison with the PVPh-*b*-PS micelles, it appeared that the P*t*BOS-*b*-PS micelles formed through solvophobic interactions of the PS blocks. Two differences in the aggregated morphologies formed between these two block copolymers arise from the relative solubility of the solvophilic blocks (i.e., the P*t*BOS block and PVPh blocks) in the same solvent and the influence of hydrogen bonding. Fig. 7 presents a series of TEM images of the aggregates of P*t*BOS_{35}-*b*-PS_{372} in acetone at different copolymer concentrations, ranging from 0.001 to 0.1 wt%. The micelles possessed spherical shape, independent of the concentration of the copolymer solution, but exhibited higher polydispersity in their sizes at higher concentrations. The morphologies of the P*t*BOS_{35}-*b*-PS_{372} system are clearly different from those of the $PVPh_{35}$-*b*-PS_{372} system, possibly due to their different chemical structures and/or the absence of hydrogen bonding in the P*t*BOS_{35}-*b*-PS_{372} system. Therefore, the hydrogen bond formation is an additional driving force that affects micelle formation in our present system. The strong intramolecular hydrogen bonding interaction of pure PVPh in linear PVPh-*b*-PS copolymer tends to form the cyclic-like copolymer, which arose from the self-assembly of ‘‘sunflower-like’’ micelles (Scheme 2).

Finally, we added the proton acceptor polymer, poly(4-vinylpyridine) into the $PVPh_{35}$-*b*-PS_{372} solution to decrease the self-association hydrogen bonding of PVPh block.

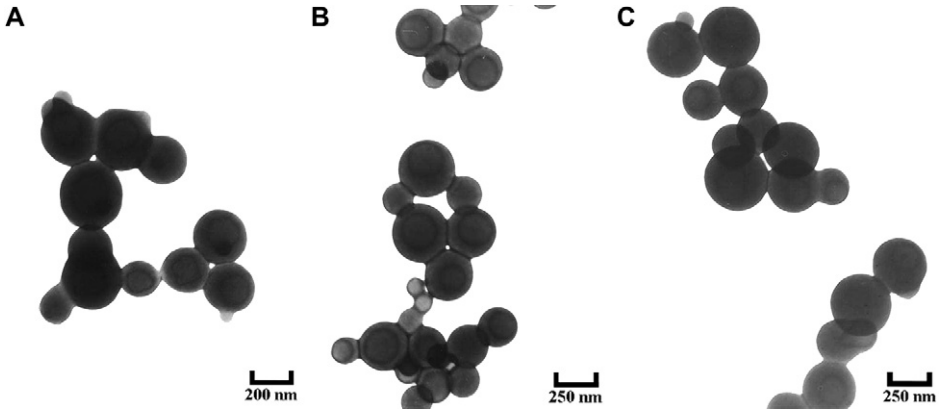

Fig. 7. TEM images of the assemblies formed from the precursor block copolymer, P*t*BOS_{35}-*b*-PS_{372}, in acetone at concentrations of (A) 0.01, (B) 0.025, and (C) 0.1 wt%.

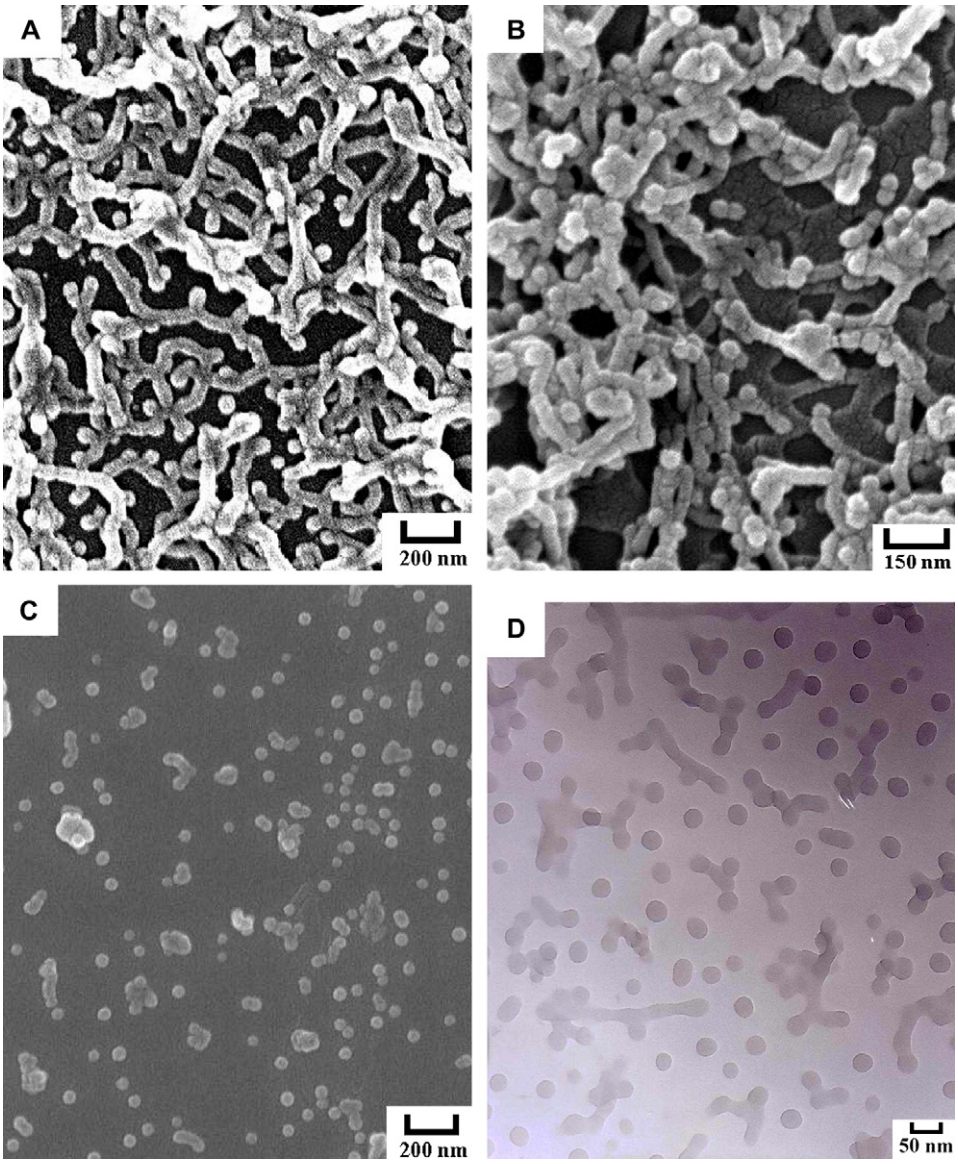

Fig. 8. Aggregates of 0.05 wt% $PVPh_{35}$-*b*-PS_{372} formed in acetone by following different volume ratios of P4VP: (A) pure $PVPh_{35}$-*b*-PS_{372}, (B) $PVPh_{35}$-*b*-PS_{372}/P4VP mixture = 10/1, (C) $PVPh_{35}$-*b*-PS_{372}/P4VP mixture = 1/1, and (D) TEM image of $PVPh_{35}$-*b*-PS_{372}/P4VP mixture = 1:1 with staining I_2.

Fig. 8A shows the morphology of the $PVPh_{35}$-*b*-PS_{372} crew-cut aggregates changing progressively from mixture worm-likes and spheres. Fig. 8B and C shows spheres and interconnected rods' mixture morphologies in $PVPh_{35}$-*b*-PS_{372}/P4VP = (10:1, v/v) blend solution by slowly adding 0.05 wt% P4VP, and mixture morphologies of spheres and short rods in 1:1 blend solution, respectively. Fig. 8D shows the TEM image at 1/1 mixtures of $PVPh_{35}$-*b*-PS_{372}/P4VP with selected P4VP domain by iodine (I_2) staining. The formation of the micelles transition is due to intermolecular hydrogen bonding between P4VP and PVPh, thus decreases or destroys the strength of self-association hydrogen bonding of PVPh block. In addition, adding P4VP will increase the area per corona chain on the core surface. As the result of breaking the hydrogen bond and surface per corona chain, the morphology changes from cylinder to sphere. Consequently, we believe that the hydrogen bonding interactions play an important role in determining the morphologies of the micelles formed from PVPh-*b*-PS copolymers in acetone solution.

4. Conclusions

We have used a single-solvent method to prepare a range of nano-objects from amphiphilic PVPh-*b*-PS block copolymers. The morphologies are easily controlled by changing, among other things, the relative length of the block copolymer and the copolymer concentration. For the shortest PVPh block, i.e., for $PVPh_{35}$-*b*-PS_{372}, the micelle changed the shape from spherical to worm-like micelles depending on the concentration of the copolymer in the acetone solution. We also observed sunflower-like $PVPh_{11}$-*b*-PS_{89} micelles that formed mainly as a result of self-associative hydrogen bonding interactions of the PVPh blocks and inter-associative hydrogen bonding interaction between PVPh with the solvent. We

further verified the importance of self-associative hydrogen bonding in this PVPh-*b*-PS/acetone system by comparing the block copolymer micelles formed from acetone solution of the $PVPh_{35}$-*b*-PS_{372} and P*t*BOS_{35}-*b*-PS_{372} copolymers, which had identical degrees of polymerization. Spherical micelles formed independent of concentration from the non-hydrogen bonding P*t*BOS_{35}-*b*-PS_{372} system are observed. In addition, adding a small amount of P4VP into PVPh-*b*-PS/acetone system will decrease the strength of self-association hydrogen bonding of the PVPh chains and result in different morphologies. Thus, it appears that strong self-associative hydrogen bonding of the coronal PVPh blocks plays an important role in dictating the resultant morphologies of the PVPh-*b*-PS copolymers in this single-solvent system.

Acknowledgment

This study was supported financially by the National Science Council, Taiwan, Republic of China, under Contract No. NSC-95-2221-E-009-166-MY3 and was also partially supported by the Ministry of Education "Aim for the Top University" program (MOEATU program).

Appendix. Supplementary data

Supplementary data associated with this article can be found in the online version, at doi:10.1016/j.polymer.2007.03.071.

References

[1] Hernandez OS, Soliman GM, Winnik FM. Polymer 2007;48:921.
[2] Foerster S, Antonietti M. Adv Mater 1998;10:195.
[3] Hoeben FJM, Jonkheijm P, Meijer EW, Schenning AP. Chem Rev 2005;105:1491.
[4] Raez J, Tomba JP, Manners I, Winnik MA. J Am Chem Soc 2003; 125:9546.
[5] Yan X, Liu G, Li Z. J Am Chem Soc 2004;126:10059.
[6] Bhargava P, Zheng JX, Li P, Quirk R, Harris FW, Cheng SZD. Macromolecules 2006;39:4880.
[7] Gao WP, Bai Y, Chen EQ, Li ZC, Han BY, Yang WT, et al. Macromolecules 2006;39:4894.
[8] Zhang LF, Eisenberg A. Science 1995;268:1728.
[9] Chatterjee U, Jwerajka SK, Mandal BM. Polymer 2005;46:10699.
[10] Zhang W, Jiang X, He Z, Xiong D, Zheng P, An Y, et al. Polymer 2006;47:8203.
[11] Chen Z, Cui H, Hales K, Li Z, Qi K, Pochan DJ, et al. J Am Chem Soc 2005;127:8592.
[12] Peng H, Chen D, Jiang M. Macromolecules 2005;38:3550.
[13] Zhang L, Eisenberg A. Polym Adv Technol 1998;9:677.
[14] Zhang L, Eisenberg A. J Am Chem Soc 1996;118:3168.
[15] Yu Y, Eisenberg A. J Am Chem Soc 1997;119:8383.
[16] Desbaumes L, Eisenberg A. Langmuir 1999;15:36.
[17] Liu L, Gao X, Cong Y, Li B, Han YC. Macromol Rapid Commun 2006;27:260.
[18] Ndoni S, Papadakis CM, Bates FS, Almdal K. Rev Sci Instrum 1995;66:1090.
[19] Li M, Douki K, Goto K, Li X, Coenjarts C, Smilgies DM, et al. Chem Mater 2004;16:3800.
[20] Zhao JQ, Pearce EM, Kwei TK, Jeon HS, Kesani PK, Balsara NP. Macromolecules 1995;28:1972.
[21] Yoshida E, Kungi S. J Polym Sci Polym Chem Ed 2002;40:3063.
[22] Yoshida E, Kungi S. Macromolecules 2002;35:6665.
[23] Jannasch P. Macromolecules 2000;33:8604.
[24] Se K, Miyawaki K, Hirahara K, Takano A, Fujimoto T. J Polym Sci Polym Chem Ed 1998;36:3021.
[25] Hadjichristidis N, Iatrou H, Pispas S, Pitsikalis M. J Polym Sci Polym Chem Ed 2000;38:3212.
[26] Lin CL, Chen WC, Liao CS, Su YC, Huang CF, Kuo SW, et al. Macromolecules 2005;38:6435.
[27] Inoue T, Chen GH, Nakamae K, Hoffman AS. J Controlled Release 1998;51:221.
[28] Wang LF, Pearce EM, Kwei TK. J Polym Sci Polym Phys Ed 1991;29:619.
[29] Coleman MM, Graf JF, Painter PC. Specific interactions and the miscibility of polymer blends. Lancaster, PA: Technomic Publishing; 1991.
[30] Sidorov SN, Bronstein LM, Kabachii YA, Valetsky PM, Soo PL, Maysinger D, et al. Langmuir 2004;20:3543.
[31] Burke SE, Eisenberg A. Langmuir 2001;17:6705.
[32] Ma Q, Remsen EE, Clark CG, Kowalewski T, Wooley KL. Proc Natl Acad Sci USA 2002;99:5058.
[33] Lei L, Gohy JF, Willet N, Zhang JX, Varshney S, Jerome R. Macromolecules 2004;37:1089.
[34] Zhang L, Eisenberg A. J Polym Sci Polym Phys Ed 1999;37:1469.
[35] Minatt E, Viville P, Borsali R, Schappacher M, Deffieux A, Lazzaroni R. Macromolecules 2003;36:4125.
[36] Quarti N, Viville P, Lazzaroni R, Minatti E, Schappacher M, Deffieux A, et al. Langmuir 2005;21:9085.
[37] Quarti N, Viville P, Lazzaroni R, Minatti E, Schappacher M, Deffieux A, et al. Langmuir 2005;21:1180.
[38] Borsali R, Minatti E, Putaux JL, Schappacher M, Deffieux A, Viville P, et al. Langmuir 2003;19:6.
[39] Brandrup J, Immergut EH. Polymer handbook. 3rd ed., vol. VII. New York: Wiley-Interscience; 1989. p. 526.
[40] Zhang WQ, Shi L, An Y, Gao LC, Wu K, Ma RJ, et al. Macromol Chem Phys 2004;205:2017.